Measurement of Young's Modulus of Vocal Folds by Indentation

Dinesh K. Chhetri, Zhaoyan Zhang, and Juergen Neubauer, *Los Angeles, California*

Summary: Objectives. To assess the accuracy of the indentation method for stiffness measurements and to estimate the Young's modulus of the vocal fold using this technique.
Study Design. Basic science.
Methods. Indentation tests were performed using a range of indenter diameters and indentation depths on single- and double-layer silicone rubber models with various cover-layer thicknesses with known geometry and Young's moduli. Measurements were repeated on intact vocal folds and isolated muscle and cover-layer samples from three cadaveric human larynges.
Results. Indentation on single-layer rubber models yielded Young's moduli with acceptable accuracy when the indentation depth was equal to or smaller than the indenter diameter, and both were smaller than the physical dimensions of the material sample. On two-layer models, the stiffness estimation was similarly influenced by indenter diameter and indentation depth, and acceptable accuracy was reached when indentation depth was much smaller than the height of the top cover layer. Measurements on midmembranous vocal fold tissue revealed location-dependent Young's moduli (in kPa) as follows: intact hemilarynx, 8.6 (range = 5.3–13.1); isolated inferior medial surface cover, 7.5 (range = 7–7.9); isolated medial surface cover, 4.8 (range = 3.9–5.7); isolated superior surface cover, 2.9 (range = 2.7–3.2); and isolated thyroarytenoid muscle, 2.0 (range = 1.3–2.7).
Conclusions. Indenter diameter, indentation depth, and material thickness are important parameters in the measurement of vocal fold stiffness using the indentation technique. Measurements on human larynges showed location-dependent differences in stiffness. The stiffness of the vocal folds was also found to be higher when the vocal fold structure was still attached to the laryngeal framework compared with that when the vocal fold was separated from the framework.
Key Words: Voice–Larynx–Viscoelasticity–Young's Modulus.

INTRODUCTION

Vocal fold vibration is determined to a large extent by the biomechanical properties of the vocal folds. The primary biomechanical property of interest in understanding self-sustained oscillation (phonation) is the stiffness (viscoelasticity) of the vocal folds.[1] The relative stiffness of the layers of the vocal folds has been shown to have a large influence on vocal fold vibration.[2–4] For detailed understanding of how vocal fold biomechanics affects phonation, accurate characterization of the material properties of the vocal folds is needed. Such an improved characterization of vocal fold biomechanics would help us to better understand phonation physics (eg, pitch control mechanisms). Clinically, a better quantification of vocal fold biomechanics would allow selection of vocal fold augmentation materials and tissue-engineered replacement constructs with the appropriate material properties.

The multilayered structure of the vocal fold consists of a deep thyroarytenoid (TA) muscle layer, an intermediate lamina propria layer, and a superficial epithelial layer. The three layers of the vocal folds have unique viscoelastic properties because of their morphological structure. The muscle layer consists of loosely packed skeletal muscle about 6 mm thick; the lamina propria is a paucicellular layer about 2 mm thick and consists mostly of extracellular matrix molecules, such as collagen and elastin, whereas the epithelial layer is a nonkeratinizing stratified squamous cell layer about 100–200 μm thick. As the epithelium is very thin compared with the lamina propria, we adopt a two-layer "body-cover" approximation of the vocal fold: the "body" layer consists of the TA muscle, and the "cover" layer comprises the lamina propria and the epithelium.[2] The TA muscle is activated under neural control and, thus, can actively change its stress state, whereas the "cover" layer has no intrinsic contractile properties, and thus, its stress state can only be changed passively by the actions of intrinsic laryngeal muscles.

There have been a few attempts to measure elastic properties of vocal fold tissue. Chan and Titze used parallel-plate rotational rheometry to measure the shear modulus of the cover layer isolated from cadaveric human larynges.[5] They found that the shear modulus ranged from 10 to 1000 Pascals (Pa). Goodyer et al measured the shear modulus by applying shear forces to the intact vocal fold surface and estimated shear moduli to be between 246 and 3356 Pa in males and between 286 and 3332 Pa in females.[6] The same method was used by Chhetri et al to measure the shear modulus of an *ex vivo* human larynx and an *in vivo* canine larynx during laryngeal nerve

stimulation.[7] They estimated the shear modulus of intact vocal folds at rest between 1076 to 1307 Pa. These latter studies measured the intact vocal fold surface and could not make the distinction between the cover and body.

Because of the small size of the larynx, in particular the thickness of the cover layer, accurate stiffness measurements using either stretching or shear rheometry are challenging, as these methods require a relatively large sample size to ensure accuracy. For small-size samples, such as biological tissues, the indentation method is often used in the measurement of material properties.[8–16] This method uses a small rigid body (indenter) to locally deform the sample surface and measures the contact force caused by imposed indenter displacements. The Young's modulus is then calculated from the slope of the force-displacement curve, based on the Hertzian contact theory of elastic bodies.[10] The indentation method was used earlier by Haji et al[8,9] to qualitatively study the relative stiffness of different regions of intact vocal folds in excised canine larynges. However, these authors did not calculate the Young's modulus.

Although the Hertzian contact theory and indentation method are suitable for use in the measurement of vocal fold stiffness, some methodological considerations need to be first addressed. In a Hertzian contact situation, the physical dimension of the material being tested is typically at least 10 times the radius of the indenter.[10] Thus, for a typical vocal fold cover layer with a thickness of 2 mm, an indenter radius of 0.2 mm or less would be desirable. However, slightly larger diameter indenters may be desirable because of improved signal to noise ratio. In addition, the effects of indentation depth on stiffness measurement are not directly addressed by Hertzian theory. Such effects are known to influence the accuracy of the estimated Young's modulus.[11] Thus, to quantitatively measure the Young's modulus of the vocal fold, the effects of experimental parameters, such as indenter diameter, indentation depth, and material thickness, need to be assessed to establish the accuracy of the experimental setup. The multilayer structure of the vocal fold also poses extra challenges for stiffness measurement. For homogeneous materials, Young's modulus can be measured in a relatively straightforward way, whereas for a multilayered structure, such as the intact vocal fold, the indentation method gives an effective modulus rather than the individual modulus of the body and cover layers. Understanding how different experimental parameters affect the estimated Young's modulus would help in choosing different experimental conditions that may allow better estimates of the stiffness of both the cover and body layers of the vocal folds.

This study attempts to provide empirical data about the Young's modulus of the vocal fold using the indentation technique. First, the accuracy of this technique was investigated using single- and double-layer silicone rubber models of various cover thicknesses and Young's moduli. The effects of experimental parameters (eg, indenter size, indentation depth, material thickness) were documented. Finally, the indentation method was used to estimate the Young's moduli of vocal folds from cadaveric human larynges in a variety of conditions (intact hemilarynx, isolated multilayered vocal fold, isolated cover, and isolated TA muscle).

METHODS

Preparation of the silicone rubber models

To study the influence of experimental parameters (indenter size, indentation depth, and material thickness), measurements were first made using single- and double-layer silicone rubber models. A two-component polymer and flexibilizer solution (Silicone rubber "Ecoflex 0010" and Silicone thinner; Smooth-On Inc., Easton, PA) at various mixing ratios of the two liquid compounds was used to make models with different Young's moduli. The Young's modulus for each model was measured using an Instron mechanical testing system (Model 5544; Instron Corp. Canton, MA). This uniaxial tensile test had an accuracy of measurement of ±5% and was used as the reference measurement for comparison with the results from indentation tests. Unless otherwise stated, the models were cubes of approximately 25.4 mm side length. To simulate the layered structure of the vocal folds and to study the influence of cover-layer thickness, two-layered models were made by curing one layer and then pouring the second layer on top of the first layer. For the two-layer models, different mixing ratios were used for each layer according to the desired modulus. For each stiffness combination, three models were made with different thicknesses of the top cover layer while keeping the combined thickness of the two layers constant (25.4 mm).

Preparation of the vocal fold tissue

The University of California Los Angeles Institutional Review Board reviewed and approved the use of donated human larynges for research. Adult human larynges were harvested from autopsy cases within 48 hours postmortem, quick-frozen, and kept at −80°C until the day before the indentation measurements. The larynx was thawed overnight at −4°C in a refrigerator and bisected at the anterior and posterior commissures to make two intact hemilarynges. Indentation experiments were performed in a variety of vocal fold tissue specimens labeled as follows: "hemilarynx" = bisected larynx with the intact vocal fold still attached to the laryngeal framework; "vocal fold" = intact vocal folds separated from the laryngeal framework by detaching at their cartilaginous attachments at the anterior commissure, vocal process, and thyroid ala; "cover" = combined vocal fold epithelium and lamina propria layers dissected and separated from the vocal fold muscle; and "muscle" = isolated TA muscle left after the "cover" layer was dissected off. Measurements were also made on a few muscle specimens that were detached from the vocal process and anterior commissure but still attached laterally to the thyroid cartilage. Samples were measured from both sides of the larynx (Table 1–3).

The muscle and cover layers were isolated by sharp scissor dissection under 3.5× loupe magnification. The isolated tissue was kept moist by spraying 0.9% saline solution and placing inside a sealed plastic bag until measurements were made. During indentation testing, tissue samples were kept at room temperature and were kept moist by submerging just to the surface in 0.9% saline solution (Figure 1). Measurements from the isolated cover layers were typically performed with the epithelium facing the indenter, unless otherwise noted in the results tables.

TABLE 1.
Estimated Young's Modulus Using the Indentation Method (Male Larynx, 49 y Old)

Sample Measured	D_{indent} (mm)	T (mm)	h_{max} (mm)	Mean $E \pm$ IQR (kPa)
Side 1				
Hemilarynx—medial vocal fold surface	0.5	—	0.8	7.4 ± 1.6
Cover—medial surface	0.5	2	0.5	5.4 ± 2
Cover—inferior medial surface	0.5	3	0.75	7.9 ± 4.6
Muscle (TA)—attached to cartilage	0.5	5	0.6	2.0 ± 2.1
Muscle (TA)—attached to cartilage	2.0	5	0.8	1.5 ± 0.8
Side 2				
Hemilarynx—medial vocal fold surface	0.5	—	0.75	5.3 ± 0.5
Muscle (TA)—attached to cartilage	0.5	5	0.75	1.3 ± 2.4
Muscle (TA)—isolated	0.5	5	0.75	2.1 ± 1.0
Muscle (TA)—isolated	1.0	5	0.75	1.6 ± 1.0

Abbreviations: D_{indent}, diameter of indenter; T, sample thickness; h_{max}, maximal depth of indentation; $E \pm$ IQR, mean Young's modulus ± interquartile range.

Measurement of loading-unloading force-displacement data

A photograph of the indentation setup is shown in Figure 1. A small cylindrical indenter was mounted onto a force transducer. The force transducer was mounted onto a motorized linear traverse (Model MA2506W1-S2.5-0; Velmex, Bloomfield, NY). The voltage from the strain gauge of the force transducer (Shimpo DF-0.5R, 220 grams load cell; Shimpo Instruments, Itasca, IL) was amplified by a factor of 100 and recorded with a PC-based AD board (UEI PowerDAQ, 16-bit resolution of 10-V input span, 2000-Hz sampling rate, UEI, Walpole, MA). The motorized linear traverse moved the cylindrical indenter at a speed of 12.7 mm/s into the sample in a direction perpendicular to the sample. Before each measurement, efforts were made to manually position the indenter as close as possible to the testing sample, without making contact. During measurements, the indenter was moved by the traverse in steps toward the testing sample (loading) and then moved back to its original position (unloading). For a maximum indentation depth of less than 2 mm, a traverse step size of 0.025 mm was used, and for maximum indentation depths of more than 2 mm a step size of 0.05 mm was used. After a wait time of 1.5 second after each traverse movement, the average of the force signal over 0.5 seconds was recorded as the indentation force (F) for the imposed indentation depth (h).

Calculation of Young's modulus (E)

For each tested sample, five loading-unloading cycles were recorded (Figure 2). The slope of the initial portion of the unloading force-indentation depth curve (dF/dh) was then estimated similar to that by Pawlak and Keller[10]: the unloading curve was fitted to a fourth-order polynomial. If the first or second derivative of the fitted function was negative, the polynomial of the next lower order was used so that both the first and second derivatives were nonnegative. Half of the data points along the unloading curve (from the start of unloading to halfway through the unloading curve) were used for this fit. The Young's modulus of the tested sample (E) was then estimated based on a Hertzian model for a cylindrical contact as follows:

$$E = \frac{1 - \nu^2}{2R}\left(\frac{dF}{dh}\right),$$

where ν is the Poisson's ratio, and R is the radius of the cylindrical indenter. Poisson's ratio is the ratio, when an object is stretched, of the transverse strain (perpendicular to the applied force) to the axial strain (parallel to the applied force) and is assumed to be 0.47 in our case for vocal fold tissue. The mean and the interquartile range (difference between the third and first quartiles) of the estimated Young's modulus are reported to indicate the accuracy of our measurements based on the five unloading curves.

TABLE 2.
Estimated Young's Modulus Using the Indentation Method (Female Larynx, 19 y Old)

Sample Measured	D_{indent} (mm)	T (mm)	h_{max} (mm)	Mean $E \pm$ IQR (kPa)
Side 1				
Hemilarynx	0.5	—	1.0	13.1 ± 1.5
Cover—superior surface	0.5	2.0	0.75	2.9 ± 1.1
Cover—medial surface	0.5	2.0	0.75	4.7 ± 1.2
Side 2				
Vocal fold—medial surface	0.5	—	1.0	3.9 ± 0.7
Vocal fold—inferior medial surface	0.5	—	1.0	7.0 ± 0.9

Abbreviations: D_{indent}, diameter of indenter; T, sample thickness; h_{max}, maximal depth of indentation; $E \pm$ IQR, mean Young's modulus ± interquartile range.

TABLE 3.
Estimated Young's Modulus Using the Indentation Method (Male Larynx, 30 y Old)

Sample Measured	D_{indent} (mm)	T (mm)	h_{max} (mm)	Mean $E \pm$ IQR (kPa)
Side 1				
Cover—superior surface	1.0	1.6	0.4	3.2 ± 1.8
Cover—medial surface	1.0	2.0	0.4	5.7 ± 2.0
Cover—medial surface, LP layer up	1.0	2.0	0.4	2.7 ± 2.3
Muscle (TA)—isolated	1.0	3.3	0.5	2.7 ± 1.5
Side 2				
Cover—superior surface	1.0	1.6	0.4	2.7 ± 1.6
Cover—medial surface	1.0	1.6	0.4	4.3 ± 1.9
Cover—medial surface, LP layer up	1.0	1.6	0.4	4.4 ± 1.9
Muscle (TA)—isolated	1.0	4.0	0.4	3.1 ± 1.4

Abbreviations: D_{indent}, diameter of indenter; T, sample thickness; h_{max}, maximal depth of indentation; $E \pm$ IQR, mean Young's modulus ± interquartile range; LP, Lamina Propria.

RESULTS
Influence of indenter size and indentation depth in single-layer silicone rubber models
Figure 3 shows the estimated Young's modulus for a one-layer rubber model as a function of indentation depth (h) for four indenter diameters (D). The Young's modulus of the model as estimated in the stretching test was 3.14 kPa. Young's modulus as estimated by the indentation method increased with increasing indentation depth and decreasing indenter diameter. As the indentation depth decreased, the estimations for all indenter sizes approached the value measured in the stretching test. Figure 3 suggests that an excessively large indentation depth compared with the indenter diameter led to large overestimation of the Young's modulus. Note that the thickness of this silicone model was 25.4 mm, which was much larger than both the indenter diameters and indentation depths used in Figure 3.

To further illustrate the effect of indenter diameter and indentation depth on modulus measurements, Figure 4 shows the normalized Young's moduli as a function of the ratio between the indentation depth (h) and the indenter diameter (D). The

Young's modulus measured by indentation (E) was normalized by the value measured in stretching-test experiment (E_0). In Figure 4, different symbols represent silicone models with different Young's moduli. A good match between E and E_0 was obtained ($E/E_0 \sim 1$) when the indentation depth was comparable or less than the indenter diameter ($h/D \leq 1$). Too large an indentation depth as compared with the indenter diameter led to significant overestimation.

Another geometric factor that may affect the measurement accuracy is the size of the material sample and its relative ratio with the indenter diameter and the indentation depth. To evaluate the influence of material thickness (T), indentation measurements were made on three single-layered silicone models with a thickness of 2, 5, and 25.4 mm (Figure 5). All three models had the same Young's modulus of 3.14 kPa as measured from stretching tests. Indenter diameters (D) of 1, 2, and 5.5 mm were used to obtain a range of ratios between the indentation
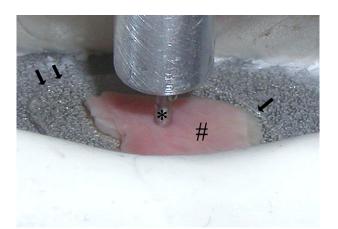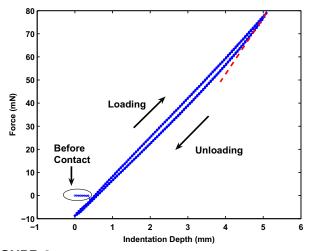

FIGURE 1. Indentation setup shows the cylindrical indenter tip (*) attached to the force transducer in contact with vocal fold tissue (#), which is placed in saline to prevent desiccation. *Arrows* point to the edge of the saline pool.

FIGURE 2. An example of the loading-unloading data over five cycles from a single-layer rubber model with material thickness = 25.4 mm, E = 3.14 kPa, indentation depth = 5 mm, and indenter diameter = 5.5 mm. The slope (dF/dh) at the initial portion of the unloading cycle (*red line*) is calculated and is used to determine Young's modulus (discussed in text).
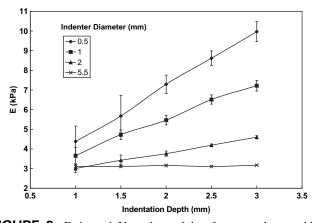
FIGURE 3. Estimated Young's modulus for a one-layer rubber model (cube with side lengths of 25.4 mm) as a function of indentation depth for four indenter diameters. The Young's modulus as estimated in the stretching test was 3.14 kPa.

depth (h) and the indenter diameter (h/D) and ratios between the indenter diameter and sample thickness (D/T). Figure 5 shows the estimated Young's moduli as a function of the ratio between the indentation depth and the indenter diameter (h/D) for various ratios of indenter diameter to material thickness (D/T). Note that the ratio h/T can be obtained from the product of the two ratios h/D and D/T. Figure 5 shows that the Young's modulus was significantly overestimated for large values of D/T ($D/T \geq 1$). For small values of D/T, more accurate estimations were obtained at small values of h/D. For the 2- and 5-mm models, Young's modulus was reasonably estimated for $D/T \leq 0.22$ and $h/D \leq 0.5$. In the 25.4-mm model, Young's modulus was accurately estimated up to h/D of 1.0 within the range of D/T between 0.04 and 0.22, which is consistent with Figure 4.

These measurements on single-layer silicone models suggest that for accurate modulus measurements using the indentation technique, the indentation depth has to be smaller than or comparable to the indenter diameter and both have to be much smaller than all physical dimensions of the material sample.
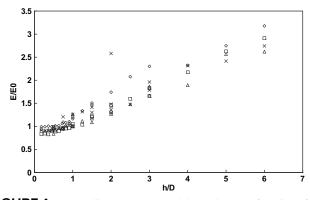

FIGURE 4. Normalized Young's modulus (E/E_0) as a function of the ratio of indentation depth (h) and indenter diameter (D). E = modulus measured by indentation and E_0 = modulus measured by stretching (Instron). Different symbols represent data from single-layer silicone models of different Young's moduli.
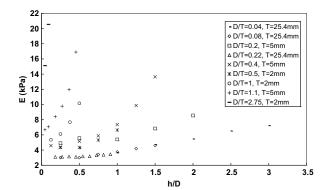

FIGURE 5. Measured Young's modulus (E) as a function of the ratio of indentation depth (h) and indenter diameter (D) for different ratios between indenter diameter and material thickness D/T. Different symbols indicate different values of the ratio D/T. Single-layer models of various thicknesses with Young's modulus 3.14 kPa were used.

Specifically, Figure 5 suggests that the experimental parameters should be selected so that conditions $D/T < 0.22$ and $h/D < 0.5$ are satisfied.

Influence of indentation depth in double-layer silicone rubber models

Figure 6 shows the estimated Young's moduli as a function of indentation depth for three different two-layer models. An indenter diameter of 1 mm was used. For all three two-layer models, the Young's moduli of the body and cover layers were 3.14 and 1.1 kPa, respectively, as measured by stretching tests (also shown in Figure 6 as solid horizontal lines). The only difference between these three models was the thickness of the cover layer of 2, 4, and 6 mm. The cover layer faced the indenter. At small indentation depths, the effective Young's modulus was closer to the Young's modulus of the cover layer than that of the body layer. The estimated Young modulus increased with increasing depth of indentation. This increase could be either because of the increasing influence of the underlying body layer, or because of the indentation depth effect as demonstrated in Figure 3. Figure 6 suggests that the stiffness of the
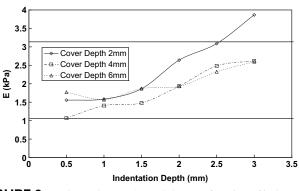

FIGURE 6. Estimated Young's modulus as a function of indentation depth for three two-layer models. The depths of the cover layers were 2, 4, and 6 mm, and indenter diameter was 1 mm. The Young's modulus as estimated in the stretching test was 3.14 kPa for body and 1.1 kPa for cover layer (represented by *solid horizontal lines*).
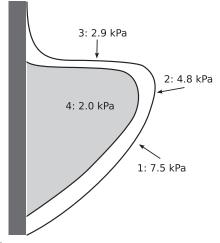
FIGURE 7. Coronal section of *ex vivo* vocal fold illustrating the order of the estimated Young's modulus from stiffest (1) to softest (4): 1 = medial inferior cover; 2 = medial cover; 3 = superior cover; 4 = TA muscle (body).

cover layer in double-layer structures may be reliably measured by using a small indentation depth compared with the depth of the cover layer. For example, in the model with a 2-mm cover layer (similar to human vocal fold cover-layer thickness), the Young's modulus of the cover layer was estimated with a slight overestimation at indentation depths smaller than 1 mm while using a 1-mm-diameter indenter.

Estimation of Young's modulus in *ex vivo* laryngeal specimens

Measurements were performed in three *ex vivo* adult human larynges using a variety of specimens (Tables 1–3). All measurements were made at the midmembranous vocal fold region or the center of the TA muscle. There was interlaryngeal variability, but the following location-dependent estimates of stiffness could be consistently discerned (N = number of specimens measured): intact hemilarynges (mean = 8.6 kPa; range = 5.3–13.1 kPa; N = 3), inferior medial surface of isolated cover (mean = 7.5 kPa; range = 7–7.9 kPa; N = 2), medial surface of isolated cover (mean = 4.8 kPa; range = 3.9–5.7 kPa; N = 5), superior surface of isolated cover (mean = 2.9 kPa; range = 2.7–3.2 kPa; N = 3), and TA muscle (mean = 2.0; range = 1.3–2.7 kPa; N = 7). These findings are illustrated in Figure 7. The stiffness estimates at the locations shown in Figure 7 were all statistically significantly different from each other (Wilcoxon rank sum test, $P < 0.05$). Several isolated muscle specimens were measured using two different indenter diameters (Table 1). Several measurements on the isolated medial surface cover layer were also made to compare differences when the epithelium faced the indenter versus the lamina propria side (Table 3). Estimated Young's modulus with lamina propria side facing the indenter (mean = 3.6 kPa; range = 2.7–4.4 kPa, N = 2) seemed slightly lower; however, the measurement errors were large.

DISCUSSION

In this study, the indentation technique was used to measure the Young's modulus of the intact vocal fold as well as isolated cover and muscle layers from *ex vivo* human larynges. The technique was first validated on silicone rubber models with known material properties, and the influence of indenter size and indentation depth was investigated. The measurements on silicone models show that the Young's modulus can be measured within a reasonable accuracy when (1) the indentation depth is smaller than the indenter diameter (Figures 3–5) and (2) both the indenter diameter and the indentation depth are much smaller than the material thickness (Figures 5 and 6). In the double-layer silicone model with a 2 mm cover layer designed to match the typical thickness of the laryngeal cover layer, the indentation technique only slightly overestimated the true Young's modulus at indentation depths of less than 1 mm when a 1-mm-diameter indenter was used (Figure 6).

Measurements in the *ex vivo* vocal fold were made following the principles learned from the silicone models, with respect to the indenter diameter and indentation depth. However, the interquartile range for our measurements was large for some specimens (Tables 1–3). This is likely because of the lower signal to noise ratio of the measurement setup for thin specimens. However, a general trend in stiffness following the morphological structure of the vocal fold could be discerned. The cover layer of the vocal fold starts at the cricoid cartilage as a membrane of connective tissue (cricothyroid membrane) and acquires the lamina propria layer about halfway along the medial surface. The superior surface is slightly thinner and also appears softer during surgical dissection. This morphological variation is likely to cause the cover-layer stiffness to be the highest at the inferior portion of the medial surface and gradually decrease toward the superior surface, which is consistent with the observations of the current study. Interestingly, the modulus of the muscle (body) layer was found to be significantly lower than that of the cover layer. Thus, in the paralyzed or denervated larynx, the cover mostly contributes to the overall stiffness of the vocal fold. Similar observation was also made by Haji et al.[8,9] They found that when the mucosa was stripped off, the stiffness of the vocal fold decreased. However, note that our measurements might only reveal the transverse Young's modulus of the muscle, whereas the longitudinal (in-fiber direction) modulus might be higher.

One vocal fold boundary condition that appears to affect estimated Young's modulus is the attachment of the vocal fold to the cartilaginous framework. The attachment of the vocal fold cover from the anterior commissure to the vocal process itself appears to increase the cover stiffness compared with the stiffness in an isolated state. Estimated Young's modulus of the vocal fold medial surface was consistently higher in the intact hemilarynx specimens compared with intact vocal folds removed from their attachments or isolated cover specimens (Tables 1–3). These findings indicate that the vocal fold is already in a slightly stretched state at rest.

Although this study sheds new light on the stiffness of the vocal fold during a nonstimulated state, it remains unclear how vocal fold moduli change with activation of various intrinsic laryngeal muscles. Ultimately, to understand the role of vocal fold stiffness changes in control of voice production, stiffness measurements should be made in an *in vivo* larynx model during neural stimulation.

CONCLUSIONS

Measurements of the Young's modulus using the indentation technique on silicone rubber models indicated that this technique is a relatively accurate method to measure vocal fold Young's modulus. For intact vocal folds, the results suggest that the indentation depth has to be limited to half the thickness of the cover layer or even smaller to obtain accurate estimates of cover-layer stiffness. Measurements on human larynges showed location-dependent differences in stiffness. The stiffness of the vocal folds was the highest in a hemilarynx setting when the vocal fold structure was still attached to the laryngeal framework. When the vocal fold was separated from the laryngeal framework and each part was isolated, the stiffness changed from the highest to the lowest from the inferior medial surface cover, the medial midmembranous cover, the superior surface cover, and finally the TA muscle.

Acknowledgment

REFERENCES

1. Titze IR. *Principles of Voice Production.* Englewood Cliffs, NJ: Prentice-Hall; 1994.
2. Hirano M. Morphological structure of the vocal cord as a vibrator and its variations. *Folia Phoniatr (Basel).* 1974;26:89–94.
3. Story BH, Titze IR. Voice simulation with a body-cover model of the vocal folds. *J Acoust Soc Am.* 1995;97:1249–1260.
4. Zhang Z. Characteristics of phonation onset in a two-layer vocal fold model. *J Acoust Soc Am.* 2009;125:1091–1102.
5. Chan RW, Titze IR. Viscoelastic shear properties of human vocal fold mucosa: measurement methodology and empirical results. *J Acoust Soc Am.* 1999;106:2008–2021.
6. Goodyer E, Hemmerich S, Müller F, Kobler JB, Hess M. The shear modulus of the human vocal fold, preliminary results from 20 larynxes. *Eur Arch Otorhinolaryngol.* 2007;264:45–50.
7. Chhetri DK, Berke GS, Lotfizadeh A, Goodyer E. Control of vocal fold cover stiffness by laryngeal muscles: a preliminary study. *Laryngoscope.* 2009;119:222–227.
8. Haji T, Mori K, Omori K, Isshiki N. Experimental studies on the viscoelasticity of the vocal fold. *Acta Otolaryngol.* 1992;112:151–159.
9. Haji T, Mori K, Omori K, Isshiki N. Mechanical properties of the vocal fold. Stress-strain studies. *Acta Otolaryngol.* 1992;112:559–565.
10. Pawlak JJ, Keller DS. Measurement of the local compressive characteristics of polymeric film and web structures using micro-indentation. *Polymer Testing.* 2003;22:515–528.
11. Cheng YT, Cheng CM. Scaling, dimensional analysis, and indentation measurements. *Mater Sci Eng Res.* 2004;44:91–149.
12. Bae WC, Lewis CW, Levenston ME, Sah RL. Indentation testing of human articular cartilage: effects of probe tip geometry and indentation depth on intra-tissue strain. *J Biomech.* 2006;39:1039–1047.
13. Delalleau A, Josse G, Lagarde JM, Zahouani H, Bergheau JM. Characterization of the mechanical properties of skin by inverse analysis combined with the indentation test. *J Biomech.* 2006;39:1603–1610.
14. Cox MAJ, Driessen NJB, Boerboom RA, Bouten CVC, Baaijens FPT. Mechanical characterization of anisotropic planar biological soft tissues using finite indentation: experimental feasibility. *J Biomech.* 2008;41:422–429.
15. Pailler-Mattei C, Bec S, Zahouani H. In vivo measurements of the elastic mechanical properties of human skin by indentation tests. *Med Eng Phys.* 2008;30:599–606.
16. Cao YP, Ma DC, Raabe D. The use of flat punch indentation to determine the viscoelastic properties in the time and frequency domains of a soft layer bonded to a rigid substrate. *Acta Biomaterialia.* 2009;5:240–248.